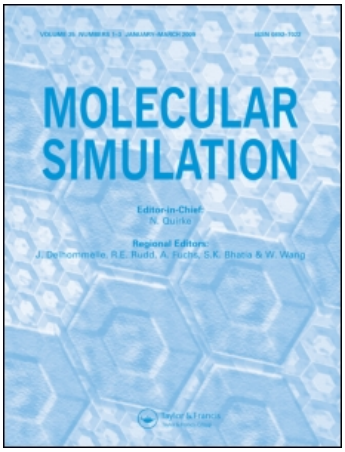

Molecular Simulation

Publication details, including instructions for authors and subscription information:
http://www.informaworld.com/smpp/title~content=t713644482

Mayer-sampling Monte Carlo calculations of methanol virial coefficients

Katherine R. S. Shaul[a]; Andrew J. Schultz[a]; David A. Kofke[a]
[a] Department of Chemical and Biological Engineering, University at Buffalo, The State University of New York, Buffalo, NY, USA

First published on: 09 November 2010

To cite this Article Shaul, Katherine R. S. , Schultz, Andrew J. and Kofke, David A.(2010) 'Mayer-sampling Monte Carlo calculations of methanol virial coefficients', Molecular Simulation, 36: 15, 1282 — 1288, First published on: 09 November 2010 (iFirst)

To link to this Article: DOI: 10.1080/08927021003699781

URL: http://dx.doi.org/10.1080/08927021003699781

Molecular Simulation
Vol. 36, No. 15, December 2010, 1282–1288

Taylor & Francis
Taylor & Francis Group

Mayer-sampling Monte Carlo calculations of methanol virial coefficients

Katherine R.S. Shaul, Andrew J. Schultz and David A. Kofke*

Department of Chemical and Biological Engineering, University at Buffalo, The State University of New York, Buffalo, NY, USA

(*Received 15 September 2009; final version received 14 February 2010*)

We present virial coefficients of up to fourth order computed by Mayer-sampling Monte Carlo for three pair potentials of methanol: one parameterised to reproduce vapour–liquid coexistence and two others parameterised to reproduce quantum-mechanical dimer energies. We compare the resulting second and third virial coefficients with experimental values available in the literature. We further examine the virial coefficients within the context of the virial equation of state, computing vapour-branch spinodals, critical points and saturated-vapour compressibility factors. The results of the three potentials differ qualitatively, reflecting the primary differences in the parameterisation schemes.

Keywords: virial coefficient; methanol; Mayer sampling

1. Introduction

The ability of an intermolecular potential to reproduce the virial coefficients B_n of the fluid it describes is an important measure of its efficacy, as these quantities encapsulate the temperature-dependent behaviour within clusters of n molecules. Connection with bulk properties is afforded by the virial equation of state (VEOS), shown in Equation (1), which relates the pressure P to the temperature T and density ρ (k is Boltzmann's constant). Analysis of the virial coefficients and properties computed from the VEOS can provide meaningful guidance as to how the molecular model could be improved.

$$\frac{P}{\rho kT} = 1 + \sum_{n=2}^{\infty} B_n(T)\rho^{n-1}. \tag{1}$$

Estimating fluid properties, such as the critical temperature, from the VEOS is trivial once the B_n values are known, but computation of these quantities remains a time-consuming task. B_n is an integral over the configuration space of the n molecules, a domain that is especially complex when the model employed is not spherically symmetric. Mayer-sampling Monte Carlo (MSMC) has enabled calculation of higher-order virial coefficients than previously possible for a variety of complex potentials, including virial coefficients of up to sixth order for several water models with fixed point charges [1] and up to fifth order for the Gaussian charge polarisable model (GCPM) of water [2].

Here, we apply the method to compute virial coefficients for three multisite pair potentials of methanol. The first model belongs to the class of transferable potentials for phase equilibria-united atom (TraPPE-UA) [3,4], which is regarded as the best available transferable model for alcohols along the saturation curve [5]. The other two models were published by Rowley, Tracy and Pakkanen (RTP) in 2006 [6] and are largely untested. To our knowledge, this is the first attempt to calculate any thermodynamic properties using the RTP methanol models.

One of the RTP methanol models includes fixed point charges as does TraPPE-UA methanol, while the other includes no electrostatic interactions. We refer to these models as RTP (PCs) methanol and RTP (no PCs) methanol, respectively. Among other differences, TraPPE-UA methanol consists of three united-atom sites and includes a bending potential, while the RTP models are rigid and have a satellite site as well as an explicit site for each atom. In addition to Coulomb interactions, sites on different TraPPE-UA methanol molecules interact through Lennard-Jones (LJ) potentials, and sites on RTP methanol models through Morse potentials.

What most differentiates the RTP methanol models from TraPPE-UA methanol is not form, but rather the way in which the parameters were fit. TraPPE-UA methanol is a semi-empirical model. Most of its parameters are borrowed from other models such as the optimised potential for liquid simulations-united atom model, while the parameters in the LJ interactions involving oxygen were optimised through Gibbs-ensemble MC (GEMC) calculations to reproduce experimental vapour–liquid coexistence curves. The RTP methanol models were developed from first principles alone: parameters of the site–site Morse potentials were optimised, in a least-squares sense, to reproduce quantum-mechanical (QM)

*Corresponding author. Email: kofke@buffalo.edu

ISSN 0892-7022 print/ISSN 1029-0435 online

DOI: 10.1080/08927021003699781
http://www.informaworld.com

dimer energies over a range of separation distances and for a variety of relative orientations.

2. Mayer-sampling Monte Carlo

MSMC has been described in detail elsewhere [1], but here we review a few key concepts. Analogous to the development of a free-energy perturbation calculation, one multiplies and divides the integral of interest Γ by a known reference quantity Γ_{ref}. Within the context of a virial-coefficient calculation, Γ_{ref} is typically chosen as the hard-sphere B_n. One then formulates the ratio of Γ to Γ_{ref} as a ratio of ensemble averages by introducing a sampling weight π. Because configurations having a larger integrand γ are more important to the calculation, π is selected to be the absolute value of γ. Singh and Kofke [7] named the method *Mayer sampling* because the integrands of virial coefficients are composed of Mayer functions. This direct-sampling formalism is summarised in Equation (2):

$$\Gamma = \Gamma_{\text{ref}} \frac{\langle \gamma/\pi \rangle}{\langle \gamma_{\text{ref}}/\pi \rangle}. \tag{2}$$

Overlap sampling was later found to be more efficient and robust when a hard-sphere reference is employed [1], and has been used in subsequent works [2,8]. It employs two sampling weights, one computed with the potential of interest and the other with the reference potential. The MSMC steps are apportioned between the two systems employed in the calculation so as to minimise the standard error. Generally, the number of steps allocated to the simulation governed by hard spheres is slightly more than 1% of the total.

Here, we employ the overlap-sampling formalism of MSMC to compute second, third and fourth virial coefficients for each methanol model at temperatures spanning a range of 275–700 K. For each temperature and order n, we employ 100 runs of one billion MC steps. Each run was performed using Java on one node of a 2×3.2 GHz Intel Xeon 'Irwindale' processor. The systems' small system size (n molecules) and short equilibration period make parallelisation trivial to implement via independent MC series.

As the order of the virial coefficient increases, so does the number of pair interaction energies that must be computed at each sampled configuration. Accordingly, one step of a B_4 calculation requires about twice as much time as one step of a B_3 calculation. Specifically, one run of one billion MSMC steps for TraPPE-UA methanol requires 10 h for B_4 and 5.5 h for B_3. For each order, runs for both of the RTP methanol models are about three times longer because of the larger number of site–site interactions required to calculate molecular interaction energies.

MSMC calculations do not employ formal bounds on configuration space. Rather, the sampling weight, which diminishes with increasing separation distances, effectively bounds the important region of configuration space. Using the absolute value of the integrand as the sampling weight, calculations of B_2 for the models with point charges employed here can, for some seeds, visit far too many configurations with long separation distances where the orientation-averaged interaction energy is negligible. Benjamin et al. [2] found that employing the absolute value of a rough orientational average of the integrand as the sampling weight, rather than the absolute value of the integrand, remedies this inefficiency [2]. The averaging introduces no approximation, as the considered orientations have equal volumes in phase space. More details regarding the method can be found in their paper, where it was applied to facilitate calculation of virial coefficients for GCPM water. Because of this procedure, one run of a B_2 calculation requires about 7 h, lasting longer than one run for B_3.

3. Results and discussion

We first present the virial coefficients computed by MSMC for each model, and we compare the B_2 and B_3 values with experimental results reported in the literature. We indirectly assess the quality of the fourth (and lower-order) coefficients by computing quantities from the VEOS that can also be compared with experimental values: namely, the critical point and the saturated-vapour compressibility factors.

3.1 Virial coefficients

The second, third and fourth virial coefficients computed by MSMC are tabulated in Tables 1–3 for TraPPE-UA methanol, RTP (no PCs) methanol and RTP (PCs) methanol, respectively. The values in parentheses are the

Table 1. Virial coefficients for TraPPE-UA methanol [3] as calculated by MSMC.

T (K)	B_2 (l/mol)	B_3 (l/mol)^2	B_4 (l/mol)^3
275	−9.4409(12)	−1851(3)	$-5.78(7) \times 10^6$
300	−4.2424(4)	−205.87(18)	$-1.004(10) \times 10^5$
325	−2.2400(2)	−33.28(3)	$-3.58(3) \times 10^3$
350	−1.33750(13)	−7.106(4)	−210.0(1.4)
375	−0.87688(6)	−1.8637(10)	−17.75(11)
400	−0.61679(3)	−0.5612(3)	−1.819(15)
425	−0.45757(2)	−0.18364(12)	−0.183(3)
450	−0.353480(16)	−0.06051(5)	0.0049(6)
475	−0.281570(14)	−0.01689(3)	0.01680(16)
500	−0.229630(9)	−0.000866(13)	0.01116(6)
550	−0.160690(6)	0.006704(6)	0.003438(10)
600	−0.117550(5)	0.006586(3)	0.001083(3)
650	−0.088273(3)	0.0054715(16)	0.0003638(13)
700	−0.067177(3)	0.0044745(10)	0.0001275(7)

Note: Numbers in parentheses represent the 67% confidence limits (standard error of the mean) for the rightmost digits of the value.

Table 2. Virial coefficients for RTP (no PCs) methanol [6] as calculated by MSMC.

T (K)	B_2 (l/mol)	B_3 (l/mol)^2	B_4 (l/mol)^3
275	−2.9040(3)	−23.644(10)	−1250(6)
300	−1.71220(14)	−5.2180(19)	−95.0(3)
350	−0.80432(4)	−0.46733(18)	−1.828(5)
400	−0.48129(2)	−0.06228(4)	−0.0936(3)
450	−0.329320(12)	−0.005591(11)	−0.00794(3)
500	−0.243840(8)	0.004106(4)	−0.000618(7)
550	−0.189660(7)	0.005354(2)	0.0001284(19)
600	−0.152400(5)	0.0049373(12)	0.0001546(11)
650	−0.125180(4)	0.0042856(8)	0.0001105(5)
700	−0.104420(4)	0.0036995(6)	0.0000785(3)

Note: Numbers in parentheses represent the 67% confidence limits (standard error of the mean) for the rightmost digits of the value.

Table 3. Virial coefficients for RTP (PCs) methanol [6] as calculated by MSMC.

T (K)	B_2 (l/mol)	B_3 (l/mol)^2	B_4 (l/mol)^3
275	−1.81160(12)	−9.252(4)	−134.4(9)
300	−1.07210(6)	−1.7985(10)	−6.58(6)
350	−0.48759(2)	−0.09011(10)	0.1030(9)
400	−0.273040(10)	0.01090(2)	0.02389(7)
450	−0.171210(7)	0.013816(7)	0.004619(12)
500	−0.114170(4)	0.010052(3)	0.000990(3)
550	−0.078493(3)	0.0071317(15)	0.0002104(13)
600	−0.054344(2)	0.0052673(10)	0.0000325(6)
650	−0.0370570(19)	0.0040952(7)	−0.0000013(3)
700	−0.0241430(18)	0.0033442(5)	0.0000007(2)

Note: Numbers in parentheses represent the 67% confidence limits (standard error of the mean) for the rightmost digits of the value.

67% confidence limits for the coefficients. Upon increasing the order of the coefficient, the ratio of this standard error to the value of the coefficient increases by about an order of magnitude given the same number of runs.

The virial coefficients differ markedly from model to model and order to order, often by several orders of magnitude, but they follow the common trend of being larger, negative and rapidly changing at low temperatures, while being smaller and slowly changing at higher temperatures. To interpolate between the values, we employ the method developed by Schultz and Kofke [9], which takes advantage of this general behaviour. We plot the simulation results along with the interpolated values in Figures 1–3 for B_2, B_3 and B_4, respectively. The coefficients are plotted on an inverse hyperbolic-sine scale to facilitate comparison across both temperature regimes on a single plot.

The differences in the parameterisation procedures for each model are clearly manifested in the calculated values of the second virial coefficient. The RTP methanol models, fit to pair information only, yield B_2 values that generally match the experimental correlation of Tsonopoulos and Dymond [10] and available experimental data

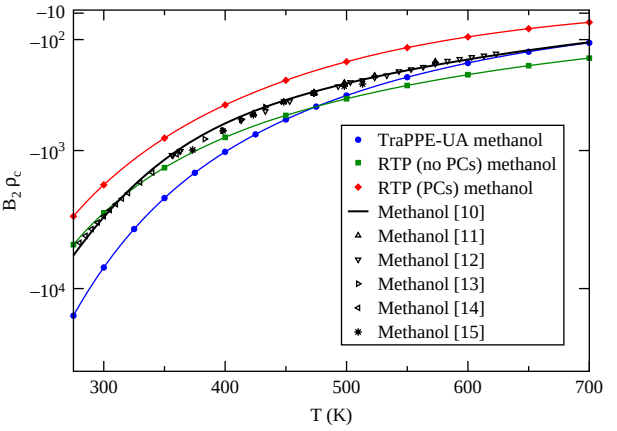

Figure 1. Temperature dependence of B_2 for each model, plotted as $\sinh^{-1}(B_2\rho_c)$ vs. temperature, where ρ_c is the experimental critical density of methanol (0.272 g/ml). Filled symbols are values computed by MSMC. Lines connecting MSMC data points were interpolated using the method of Schultz and Kofke [9]. Open symbols are experimental data [11–15].

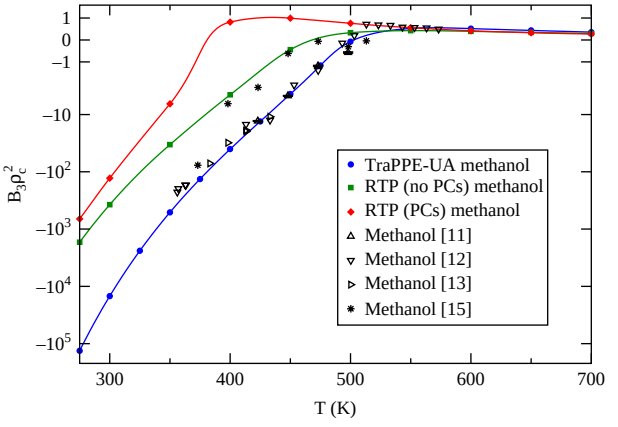

Figure 2. Temperature dependence of B_3 for each model, plotted as $\sinh^{-1}(B_3\rho_c^2)$ vs. temperature. Filled symbols are values computed by MSMC. Lines connecting MSMC data points were interpolated using the method of Schultz and Kofke [9]. Open symbols are experimental data [11–13,15].

[11–15] more closely than B_2 values computed for TraPPE-UA methanol. TraPPE-UA methanol is parameterised to reproduce bulk liquid–vapour coexistence data, such that multibody effects are accounted for in the pair potential.

At the lower temperatures considered, the B_2 values of RTP (no PCs) methanol are particularly good. This result raises concerns about the quality of the Coulomb potentials of the other models, as strongly directional interactions are more significant at lower temperatures. We note that in the plots of the RTP and QM potential energies published by Rowley et al. [6], one can see that the RTP (no PCs) potential is generally much weaker than both the QM and the RTP (PCs) potentials at separation distances larger than 6 Å, not a particularly long separation distance considering

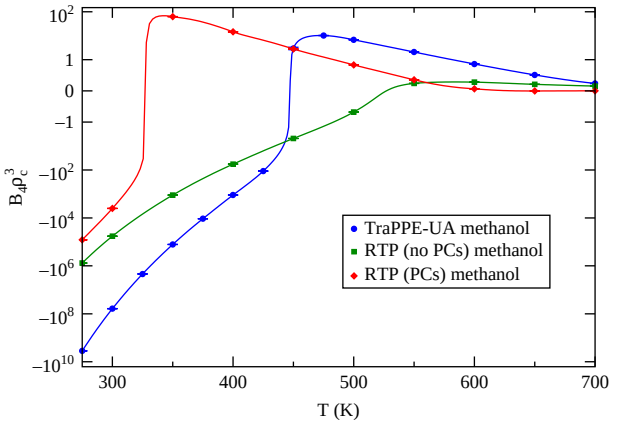

Figure 3. Temperature dependence of B_4 for each model, plotted as $\sinh^{-1}(10B_4\rho_c^3)$ vs. temperature. Filled symbols are values computed by MSMC. Lines connecting MSMC data points were interpolated using the method of Schultz and Kofke [9].

the well depths. Still, this marked weakness is likely a result of the absence of Coulomb site–site potentials, which would persist at larger separation distances than LJ or Morse interactions.

Analogous to how Boltzmann averages of a dipole–dipole interaction energy over relative orientations are more attractive at lower temperatures (configurations that minimise the potential energy are more favoured), the inclusion of appropriate orientation-dependent electrostatic interactions should make the virial coefficients more negative at lower temperatures. As the temperature increases, the sampling of orientations becomes more random, mitigating this effect for a model with strongly directional interactions such as the Coulomb interactions of TraPPE-UA methanol.

The fixed point charges of TraPPE-UA methanol result in a dipole moment of 2.23 D at the equilibrium bond angle. This and its other parameters are selected to strike a balance between vapour and liquid properties, inevitably resulting in a pair interaction energy that is too attractive to describe interactions in the vapour accurately. Thus, it is not surprising that the B_2 values of TraPPE-UA methanol are too negative over much of the temperature range, but improve with increasing temperature. Benjamin et al. [1] observed the same B_2 behaviour in their examination of water models with fixed point charges parameterised in a similar fashion.

The second virial coefficient of RTP (no PCs) methanol is appropriate at the lower temperatures but becomes too negative as temperature increases, perhaps because the potential is less sensitive to orientation. Indeed, the virial coefficients of RTP (no PCs) methanol and TraPPE-UA methanol cross paths between 450 and 525 K, implying that the potential of TraPPE-UA methanol is more attractive than that of RTP (no PCs) methanol at configurations important at lower temperatures, and more repulsive at configurations important at higher temperatures.

RTP (PCs) methanol yields markedly more positive coefficients than the other models at all orders considered, and it is clearly the potential with the most overall repulsive nature. It employs a distribution of point charges with a dipole moment of 2.07 D, a value 7% smaller than the dipole moment of relaxed TraPPE-UA methanol, which explains, at least in part, why the B_n values of RTP (PCs) methanol are more positive than those of TraPPE-UA methanol. It is more difficult to understand why the B_n values of RTP (PCs) methanol are more positive than those of experiment and RTP (no PCs) methanol. In the plots published by Rowley et al. [6], the potential of RTP (PCs) methanol is consistently more repulsive than that of RTP (no PCs) methanol for routes in which the oxygen sites approach one another, but other approach routes yield mixed results. The dipole moment of RTP (PCs) methanol is larger than the value of 1.70 D determined experimentally for methanol vapour [16], but we do not know what values are appropriate for strongly interacting methanol dimers. If the Coulomb potentials are, on average, too attractive, the Morse contribution must be overcompensating for it.

The agreement of B_3 between 400 and 500 K for TraPPE-UA methanol and methanol [11–13] is remarkable. At these and lower temperatures, B_3 values for TraPPE-UA methanol are even larger relative to the RTP values than was the case for B_2, and the difference is amplified further at fourth order. This amplification of the difference with increasing order is a simple result of the accompanying increase in the number of pair interactions.

3.2 *Vapour-branch spinodals and critical points*

From the third- and fourth-order virial equations of state (VEOS3 and VEOS4), we compute spinodal curves for each potential up to the critical point, plotted in Figure 4. We do not do the same for VEOS3 of methanol, due to the

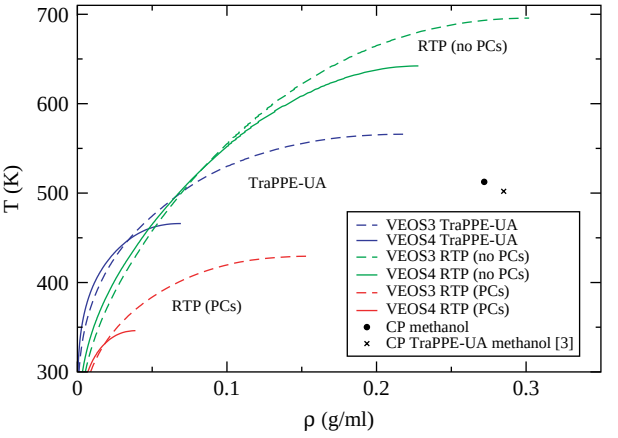

Figure 4. Spinodals computed from VEOS3 and VEOS4 for each model up to the computed critical point.

amount of scatter in the experimentally determined B_3 values. We do not plot any part of the liquid branch of the spinodal because it is often inaccurate to the point of being unphysical; the inapplicability of the VEOS to the liquid phase prevents computation of the binodal as well. We include the critical point of methanol, determined experimentally, and the critical point of TraPPE-UA methanol, determined through GEMC and scaling arguments [3]. To our knowledge, the critical points of the RTP models have not been computed, nor have other spinodal points of any of the models we consider.

The spinodals computed from the truncated VEOSs differ greatly from model to model, reflecting the differences in the virial coefficients. RTP (PCs) methanol, which has the most positive virial coefficients, yields significantly lower spinodal temperatures, consistent with the expectation that a more repulsive potential would yield vapour metastable at lower temperatures. Similar to the behaviour observed for the virial coefficients, the VEOS3 and VEOS4 spinodals of RTP (no PCs) methanol and TraPPE-UA methanol cross paths between 450 and 500 K.

For models of simple fluids, such as the LJ potential, low-order VEOSs can yield reasonable estimates of the critical temperature. For example, VEOS4-LJ yields a critical temperature within 1% of the correct value [17]. By contrast, VEOS4 of TraPPE-UA methanol underestimates the critical temperature of the model, 502(2) K [3], by 7.2%. Poorer agreement for a particular order of VEOS is to be expected for models of associating fluids, as higher-order interactions are more important. With that caveat noted, our low-order estimates indicate that RTP (no PCs) methanol would likely overpredict the critical temperature of methanol, while RTP (PCs) methanol would underpredict it.

3.3 *Saturated-vapour compressibility factors*

We compute VEOS approximations to the compressibility factor Z along the vapour branch of the binodal as this provides us with another means of gauging the models' accuracies: the liquid–vapour coexistence curve has been determined by experiment for methanol [18,19] and by GEMC for TraPPE-UA methanol [3]. In Figure 5, we plot the resulting Z values, as well as those computed from truncated VEOSs for each model and methanol.

The VEOS Z values for methanol employ the B_2 and B_3 values of Bich et al. [12], available at 356.15 K and higher, as well as the B_2 values of Boyes et al. [14], which extend the temperature range of VEOS2 down to 280 K. The VEOS Z values of methanol and the RTP models were computed assuming the saturation temperatures and vapour densities determined for methanol by experiment, while those of TraPPE-UA methanol were computed assuming the saturation temperatures and vapour densities determined for the model by GEMC. Only the standard

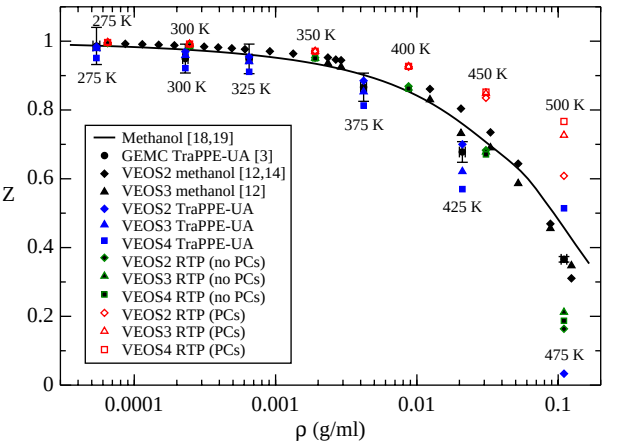

Figure 5. Compressibility factors computed along the saturated vapour line.

Notes: Compressibility factors for VEOS*n*-TraPPE-UA methanol were computed assuming the saturated vapour densities and temperatures determined for TraPPE-UA methanol by GEMC. The saturation temperatures are listed beneath the data. Compressibility factors for VEOS*n* of both RTP models were computed assuming the NIST saturated vapour densities and temperatures of methanol [18,19]. The saturation temperatures are listed above the data. The uncertainties in the computed compressibility factors resulting from standard errors in the computed virial coefficients are smaller than the markers employed.

errors in the virial coefficients, and not the standard errors in the GEMC saturated-vapour densities, are used to compute the confidence limits of the VEOS*n* compressibility factors. These confidence limits are smaller than the markers employed.

At the lower densities and temperatures, VEOS Z values of RTP (no PCs) methanol reproduce the Z values of methanol the best, reflecting the good agreement between the B_2 values of the model and methanol at low temperatures. Below 400 K, there is strong agreement (to within about 0.2%) between the results of the different orders of VEOS for each of the RTP models, indicating that third- and fourth-order contributions are minute. From the two experimental VEOS3 Z values between 350 and 400 K, one can see that the RTP models underestimate the third-order contribution there.

At the smallest densities considered, where the experimental VEOS2 results agree quite well with the bulk, one would not anticipate significant contributions from higher-order terms. However, even at the lowest density, the fourth-order contribution of TraPPE-UA methanol is non-negligible: the fourth-order compressibility factor differs from the second-order result by more than 3%, a difference that is too large to be the result of standard error. At the three lowest densities, all of the VEOS Z values for TraPPE-UA methanol lie within the error bars of the GEMC data, but the VEOS4 results appear to diverge from the GEMC data, indicating that even higher-order contributions could be significant at these densities. The only positive virial coefficient for

TraPPE-UA methanol at the saturation conditions considered is B_4 at 475 K, such that all of the other values serve to reduce the compressibility factor. Presumably, higher-order coefficients become positive at lower temperatures.

As the density increases, the VEOS Z values of the RTP models diverge from the experimental results. At the highest density considered, VEOS4 of TraPPE-UA methanol provides the best estimate of the experimental Z, but the value is outside the error bars of the GEMC result. At this density, the VEOS2 and VEOS3 results for TraPPE-UA methanol are highly inaccurate. In particular, the VEOS3 Z value corresponds to a negative pressure and is off the scale of the plot.

The GEMC results for TraPPE-UA methanol yield compressibility factors that are always smaller than those of methanol, which is another indication that the potential is too attractive. Similarly, the VEOS Z values of RTP (PCs) methanol are all too high, reflecting a potential that is too repulsive. The transition in the VEOS Z of RTP (no PCs) methanol from being too high to too low occurs between 400 and 450 K; intersection with Z values of TraPPE-UA methanol would appear to occur at higher temperatures.

4. Conclusions

The virial coefficients consolidate the spatial dependence of the potentials considered, conclusively demonstrating that RTP (PCs) methanol is, overall, more repulsive than both methanol and the other models at relevant configurations. RTP (no PCs) methanol appears to generally reproduce the best experimental values at low temperatures and densities, but its poorer performance at higher temperatures is likely caused by the absence of electrostatic interactions of some type. Across the range of temperatures considered, the results for TraPPE-UA methanol reflect a pair potential that is too attractive.

The significant fourth-order contribution of TraPPE-UA methanol to the saturated-vapour compressibility factor at densities three orders of magnitude smaller than the critical density is unphysical but not unexpected for a model with fixed point charges developed to reproduce vapour–liquid coexistence. The inaccuracy of the compressibility factors computed from VEOS2 and VEOS3 of TraPPE-UA methanol at the highest density point considered reflects more poorly upon VEOS2 and VEOS3 than it does upon the model. Generally, the more important multibody interactions are, the less effective a low-order VEOS is.

Although TraPPE-UA methanol overpredicts the importance of multibody interactions at the conditions considered, both RTP methanol models appear to underpredict their importance. This underprediction is likely a direct result of their parameterisation employing QM potential energies of pairs and not higher-order clusters. However, the large differences in the results of the two RTP models demonstrate the difficulty of developing effective pair potentials from a dimer QM potential energy surface, and diminish the appeal of applying the fitting procedure to the even more complex surfaces of higher-order clusters. Because of the severity of the differences in the results of the two RTP models, we can conclude little from this work about the quality of the QM potential employed to develop them.

Virial coefficients could facilitate a more systematic approach to the parameterisation of potentials from QM data. Acknowledging current computational barriers, virial coefficients seamlessly connect molecular-level detail with bulk vapour behaviour, and they can be compared directly with experimental data at low orders. Most interestingly, within the context of Mayer sampling, the virial coefficients provide quantitative guidance as to what part of the QM potential energy surface would be most important to reproduce for application of the fitted potential at a particular temperature.

Acknowledgements

Funding for this research was provided by Grant CHE-0626305 from the US National Science Foundation, and by the University at Buffalo School of Engineering and Applied Sciences. Computational support was provided by the University at Buffalo Center for Computational Research.

References

[1] K.M. Benjamin, J.K. Singh, A.J. Schultz, and D.A. Kofke, *Higher-order virial coefficients of water models*, J. Phys. Chem. B 111 (2007), pp. 11463–11473.

[2] K.M. Benjamin, A.J. Schultz, and D.A. Kofke, *Fourth and fifth virial coefficients of polarizable water*, J. Phys. Chem. B 113 (2009), pp. 7810–7815, Erratum: DOI: 10.1021/jp101381c.

[3] B. Chen, J.J. Potoff, and J.I. Siepmann, *Monte Carlo calculations for alcohols and their mixtures with alkanes. Transferable potentials for phase equilibria. 5. United-atom description of primary, secondary, and tertiary alcohols*, J. Phys. Chem. B 105 (2001), pp. 3093–3104.

[4] M.G. Martin and J.I. Siepmann, *Transferable potentials for phase equilibria. 1. United-atom description of n-alkanes*, J. Phys. Chem. B 102 (1998), pp. 2569–2577.

[5] N. Ferrando, V. Lachet, J.-M. Teuler, and A. Boutin, *Transferable force field for alcohols and polyalcohols*, J. Phys. Chem. B 113 (2009), pp. 5985–5995.

[6] R.L. Rowley, C.M. Tracy, and T.A. Pakkanen, *Potential energy surfaces for small alcohol dimers I: Methanol and ethanol*, J. Chem. Phys. 125 (2006), 154302.

[7] J.K. Singh and D.A. Kofke, *Mayer sampling: Calculation of cluster integrals using free-energy perturbation methods*, Phys. Rev. Lett. 92 (2004), 220601, Erratum: ibid, 95 (2005), 249903.

[8] K.M. Benjamin, A.J. Schultz, and D.A. Kofke, *Virial coefficients of polarizable water: Applications to thermodynamic properties and molecular clustering*, J. Phys. Chem. C 111 (2007), pp. 16021–16027.

[9] A.J. Schultz and D.A. Kofke, *Interpolation of virial coefficients*, Mol. Phys. 107 (2009), pp. 1431–1436.

[10] C. Tsonopoulos and J.H. Dymond, *Second virial coefficients of normal alkanes, linear 1-alkanols (and water), alkyl ethers, and their mixtures*, Fluid Phase Equilibr. 133 (1997), pp. 11–34.

[11] G.S. Kell and G.E. McLaurin, *Virial coefficients of methanol from 150 to 300°C and polymerization in the vapor*, J. Chem. Phys. 51 (1969), pp. 4345–4352.
[12] E. Bich, R. Pietsch, and G. Opel, *Second and third virial coefficients of methanol vapor*, Z. Phys. Chem. (Leipzig) 265 (1984), pp. 396–400.
[13] G. Olf, A. Schnitzler, and J. Gaube, *Virial coefficients of binary mixtures composed of polar substances*, Fluid Phase Equilibr. 49 (1989), pp. 49–65.
[14] S.J. Boyes, M.B. Ewing, and A.R.H. Goodwin, *Heat-capacities and 2nd virial-coefficients for gaseous methanol determined from speed-of-sound measurements at temperatures between 280 K and 360 K and pressures from 1.03 kPa to 80.5 kPa*, J. Chem. Thermodyn. 24 (1992), pp. 1151–1166.
[15] A.N. Shakhverdiev, Y.M. Naziev, and D.T. Safarov, *Densities of aliphatic alcohol vapors*, Teplofiz. Vys. Temp. 31 (1993), pp. 369–372.
[16] D.R. Lide, *CRC Handbook of Chemistry and Physics, 89th Edition (Internet Version 2009)*, CRC Press, Boca Raton, FL, 2008–2009.
[17] A.J. Schultz and D.A. Kofke, *Sixth, seventh, and eighth virial coefficients of the Lennard Jones model*, Mol. Phys. 107 (2009), pp. 2309–2318.
[18] K.M. de Reuck and R.J.B. Craven, *Methanol, international thermodynamic tables of the fluid state – 12*, IUPAC, Blackwell Scientific Publications, London, 1993.
[19] A. Polt, B. Platzer, and G. Maurer, *Parameter der thermischen Zustandsgleichung von Bender fuer 14 mehratomige reine Stoffe*, Chem. Tech. (Leipzig) 44 (1992), pp. 216–224.